U. S. DEPARTMENT OF COMMERCE
NATIONAL OCEANIC AND ATMOSPHERIC ADMINISTRATION
NATIONAL WEATHER SERVICE
NATIONAL CENTERS FOR ENVIRONMENTAL PREDICTION

OFFICE NOTE 428

Impact of the subgrid representation of parameterized convection on simulated climatology

SONG-YOU HONG
GENERAL SCIENCES CORPORATION

January 2000

Corresponding author address : Dr. Song-You Hong, NCEP/EMC, Room 207
5200 Auth Road, Camp Springs, MD 20746
E-mail : Songyou.Hong@noaa.gov

Abstract

The sensitivity of general circulation models (GCMs) to the subgrid representation of parameterized convection is investigated. Various experiments testing the sensitivity of the simulated climatology to parameters in convective downdrafts were conducted within the framework of a perpetual January run. The mass flux of the parameterized downdraft is varied in magnitude up to the maximum value allowed within the current parameterization framework over the ocean, while over land it is bounded to a specific value. This concept is based on the fact that soil temperature and moisture over land are highly correlated to the amount of parameterized convective precipitation, whereas over the ocean the corresponding subsurface properties in the model are prescribed by the sea surface temperature. The impact of enhanced evaporation of precipitation over the oceans was also discussed. The sensitivity experiment was extended to an ensemble simulation framework for two different summers and winters, in terms of SST over the tropical oceans.

The modified scheme with an maximum downdraft over the ocean clearly shows improvements compared to that from the convection scheme with a suppressed downdraft. The modified scheme suppresses the erroneously excessive rainfall north of the equator and increases rainfall over the Southern Hemispheric oceans, which generally agrees better with the observed January precipitation climatology. The improvement is also significant in the low-level wind distribution, particularly easterlies over the equatorial Pacific between 130-160 W, which are too weak in the operational version of the scheme. Enhanced evaporation shows comparable impact to modified downdrafts in that both effects play a role in stabilizing the atmosphere. Ensemble simulations with it, for January of 1997 and 1998, reveal consistent improvement in precipitation anomalies as achieved in the perpetual run. The improvement of simulated precipitation anomalies for July of 1996 and 1997 is also significant in response to SST anomalies over the tropical oceans.

1. Introduction

The National Centers for Environmental Prediction (NCEP) operational Medium-Range Forecast (MRF) model has, in recent years, shown considerable improvement in the skill of short and medium range forecasts, as measured by global anomaly correlation scores and precipitation skill scores over the United States. Some of the improvements can be attributed to improved physics introduced into the model, including convective precipitation processes, surface layer and turbulence schemes (Hong and Pan 1996, Caplan et al. 1997). However, for tropical rainfall climatology the model seems inferior to the current climate model used at NCEP (Kumar et al. 1996), which is based on both the operational MRF model as of 1991 and a Kuo convection scheme tuned to sea surface temperature (SST). The most serious problems in the operational MRF model as of January 1998 occur in the Northern Hemisphere winter, and are excessive precipitation related to the Inter-Tropical Convergence Zone (ITCZ) north of the equator and underprediction of warm pool precipitation in the Southern Hemisphere (Masutani 1997).

This study attempts to address these deficiencies in the representation of the precipitation climatology by investigating the representation of parameterized convection in the MRF. Previous studies have shown a significant sensitivity of simulated climatology to the representation of deep convection in the cumulus parameterization scheme of GCMs (e.g., Zhang, 1995, Baik and Takahashi 1995, Ridout and Reynolds 1998). Zhang (1995) demonstrated the sensitivity of surface fluxes to the choice of convection parameterization scheme. Baik and Takahashi (1995) found a great sensitivity of simulated climatology to the convective adjustment time scale in a convection scheme. Ridout and Reynolds (1998) improved the warm pool precipitation by introducing a convective triggering function associated with the presence of the boundary layer thermals.

In cumulus clouds, downdrafts cool and dry the lower troposphere and consume cloud and rain water through evaporation. Since Johnson (1976) first attempted to include the downdraft effects in cumulus diagnosis, various efforts have been made to come up with a reasonable method of parameterizing downdrafts (e.g., Fritsch and Chappell 1980, Molinari and Corsetti 1985, Frank and Cohen, 1987, Grell 1993, Cheng and Arakawa 1997, Spencer and Stensrud 1998). The importance of the convective downdraft in the cumulus parameterization scheme is relatively well established in mesoscale models (e.g., Zhang and Gao 1989, Grell 1993, Wang and Seaman 1997). For example, Zhang and Gao (1989) demonstrated that the convective downdraft is one of the key mechanisms in reproducing the cooling and moistening of below-cloud layers, which results in the subsequent development of organized convective clouds over the central Great Plains. The representation of the convective downdraft in a mesoscale model has been further shown to improve quantitative precipitation forecasts (e.g., Wang and Seaman 1997, Spencer and Stensrud 1998). However, in low resolution global models, used for climate studies, the sensitivity of model performance to variations in parameterized downdraft formulation has not been demonstrated.

This study examines the importance of subgrid representation of parameterized convection, based on a simple idea that differences in land surface -atmosphere interaction over ocean and land may require different downdraft properties in the cumulus parameterization scheme. Sensitivity of climate simulations to the representation of convective downdrafts and evaporation of precipitation are conducted within the framework of perpetual January runs using a T40 resolution (triangular truncation at wave number 40, approximately 300 km). The results

are interpreted against observed climatology. Experiments are extended to an ensemble simulation framework with a T62 model (approximately 200 km), for two winters and summers. Experimental designs, including the background of the relaxed downdrafts in the convective parameterization scheme, are described in section 2, together with a brief description of the MRF model. The results are discussed and interpreted in section 3. Concluding remarks are given in section 4.

2. Experimental designs

a. The MRF model

The NCEP MRF model is a global spectral model (Sela 1980). Subsequent developments of the model are described in Kanamitsu (1989), Kanamitsu et al. (1991), Hong and Pan (1996), and Caplan et al.(1997). The model physics include long-and short- wave radiation, cloud-radiation interaction, planetary boundary-layer processes, deep and shallow convection, large-scale condensation, gravity wave drag, enhanced topography, simple hydrology, and vertical and horizontal diffusions. The MRF model uses a two-layer soil model (Pan and Mahrt 1987), which includes both soil thermodynamics and soil hydrology, modeled as diffusion processes. The evaporation process in the surface energy balance is modeled as three components: direct evaporation from the bare soil surface, transpiration through the leaf stomata, and re-evaporation of intercepted precipitation by the leaf canopy. The boundary layer physics employs a nonlocal diffusion concept (Hong and Pan 1996). This scheme is strongly coupled to the surface layer physics. In the scheme, the turbulent diffusivity coefficients are calculated from a prescribed profile shape as a function of boundary-layer heights and scale parameters derived from similarity requirements. Above the mixed layer, the local diffusion approach is applied to account for free atmospheric diffusion.

Except for resolution differences, the model used in this study is the same as the operational MRF model as of January 1998. The model employs a resolution of T40/L18 (triangular truncation at wave number 40 in the horizontal and 18 terrain-following sigma layers in the vertical) for the perpetual runs, and T62/L28 for the ensemble simulations which is lower than the T126/L28 used for routine daily forecasts.

b. Precipitation physics

Precipitation is produced by both large-scale condensation and the convective parameterization schemes. The large-scale precipitation algorithm checks for supersaturation in the predicted specific humidity field. Latent heat is released as the specific humidity and temperature are adjusted to saturation values. The scheme does not include a prognostic cloud, but does account for evaporation of rain in the unsaturated layers below the level of condensation.

The current version of the deep convection scheme follows Pan and Wu (1995), which is further based on Arakawa and Schubert (1974), as simplified by Grell (1993). Recent improvements to the scheme are discussed in Hong and Pan (1996), where convection is allowed in disturbed atmospheric conditions when the convectively available potential energy (CAPE) is large. The primary differences between Pan and Wu (1995) and Grell (1993) lie in the closure (the NCEP scheme uses the original Arakawa-Schubert closure) and the treatment of below-cloud layers (the NCEP scheme allows entrainment of updraft and detrainment of downdraft between the updraft-air originating level and the level of free convection (LFC)). In the scheme, the mass

flux of the cloud is determined using a quasi-equilibrium assumption based on a threshold cloud work function deduced from observations (Lord 1978). The level of maximum moist static energy between the surface and 400-hPa level from the surface is used as the originating level for updrafts. The LFC is the cloud base. Cloud top is defined as the first neutral level above the cloud base. Downdraft and re-evaporation of precipitation in the convection scheme are described below.

A saturated downdraft is assumed as in Grell (1993), but the downdraft detrains below cloud base. The downdraft mass flux, m_0, is represented as a fraction of the updraft mass flux, m_b ,

$$m_0 = \frac{\beta I_1 m_b}{I_2} \qquad (1)$$

where I_1 represents the amount of condensation integrated over the whole depth of the updraft normalized by the updraft mass flux, and I_2 the amount of the evaporation of condensate in the downdraft, and the parameter β specifies the fraction of updraft condensate that evaporates in the downdraft. The precipitation rate due to the updraft and downdraft couplet at a level, z, is computed from the cloud top downward and given by

$$R(z)_{conv} = \eta_u(z) c_0 q_l(z) m_b - \eta_d(z) q_e(z) m_0 \qquad (2)$$

where η_u and η_d are the normalized updraft and downdraft mass flux fraction, respectively. Entrainment of the updraft air and detrainment of the downdraft air are tuned so that the updraft mass flux doubles as the parcel rises from the starting level to the cloud base and is assumed to be constant in the cloud layer. Downdraft mass flux decreases from 1 to 0.05 as it descends from cloud base to the surface. The factor c_0 is a rainfall conversion parameter, q_l is the suspended cloud liquid water, and q_e the amount of moisture that necessary to keep the downdraft saturated.

The factor β in (1) is the downdraft efficiency, which is derived following Fritsch and Chappell (1980). The precipitation efficiency (1-β) is parameterized as a function of the vertical wind shear within a cloud (Fig. 1), and is expressed by the following equation :

$$1-\beta = 1.591 - 0.639S + 0.0953S^2 - 0.00496S^3 \qquad (3)$$

where S is the averaged vertical shear of the horizontal wind between cloud base level and maximum wind level below cloud top, and has units of $10^{-3} s^{-1}$. β is bounded at zero when S becomes small. Note that, for the MRF, the wind shear between the cloud base and the maximum wind level is used to compute precipitation efficiency as done in Zhang and Fritsch (1986), rather than the shear over the total cloud depth as originally proposed by Fritsch and Chappell (1980). From (1)-(3), it can be seen that a strong vertical wind shear reduces the amount of parameterized convective rainfall by creating an enhanced downdraft.

The re-evaporation of convective precipitation in (2) is considered if the environmental air is unsaturated, and it is given by

$$R(z) = R(z)_{conv} - R(z)_{evap} [\equiv -\alpha \Delta q \times \{1 - e^{\left(-0.32 \Delta t \sqrt{R(z)_{conv}}\right)}\}] \qquad (4)$$

The rate $R(z)_{evap}$ is adopted from the formula in the grid-resolvable precipitation physics (NMC 1988) following the form of Kessler (1969), Δt is the model time step, and Δq is the supersaturation mixing ratio (kg/kg-1), which is less than zero. The evaporation efficiency, α, is a constant or the function of the vertical wind shear as in the downdraft efficiency in (3).

Note that these parameterizations have been tuned for daily weather forecasts. For example, precipitation efficiency in (3) can range from 0 to 1, depending on the magnitude of vertical wind shear, but in the model it is bounded to the lower limit of 0.7 (β varies between 0 and 0.3), even in the case of strong wind shears. Furthermore, the impact of re-evaporation of convective precipitation is very weak (α=0.07 in (4)). This treatment is necessary to achieve a realistic amount of precipitation in MRF, and is discussed further in the next section.

c. Background of convective downdraft and experimental setup

Xu and Arakawa (1992) showed that the inclusion of convective-scale downdrafts results in significant stabilization of the below-cloud layer, which in turn influences the intensity of the subsequent parameterized cumulus convection. They attribute this to the cooling in the below-cloud layer by the downdraft. They also demonstrated that this stabilization effect becomes smaller as the horizontal averaging distance decreases. Their results imply that downdraft efficiency may need to be changed in low resolution models in order to obtain realistic precipitation amounts. Giorgi et al. (1993) investigated the sensitivity of the downdraft efficiency in a regional climate model having a horizontal resolution of 50 km and found that the efficiency should be no more than 0.5. Other evidence is found in Wang and Seaman (1997), who suppressed the downdraft efficiency to correct the problem associated with underestimation of convective precipitation in a mesoscale model with a grid size of 12 km. A comprehensive study is found in Spencer and Stensrud (1998), who examined the sensitivity of precipitation forecasts to the treatment of convective downdrafts and the magnitude of precipitation efficiency in the Kain and Fritch scheme (1990). They demonstrated that precipitation appears to be very sensitive to the way downdrafts are treated within the convection scheme. They also showed that maximizing rainfall by forcing the precipitation efficiency to 0.9 provides modest improvement in the simulated rainfall fields. To achieve reasonable skill score in MRF daily quantitative precipitation forecasts, the downdrafts are suppressed, with the maximum efficiency (β in the previous section), set to 0.3 over land and ocean.

Recent testing has indicated, however, that while the implementation of this upper bound in downdraft efficiency may lead to better simulations over land areas, it may be detrimental to predictions over the water. The discrepancy between land and water grid points appears to be due to the fact that parameterized surface-atmospheric interactions over land areas are more complex and more dependent on parameterized convective feedbacks than over open water. In particular, over land the soil moisture and temperature values must be calculated by solving a full system of parameterized equations at the surface. These equations involve the surface energy budget, which in turn is strongly influenced by precipitation and cloud amounts in the parameterized convection. In contrast, over the oceans, the surface boundary condition represented by the SST is well known to play a major role in forcing the atmosphere, and understanding its role has been a simpler task, both because SST is observed daily and because the surface is saturated at this temperature. A comprehensive description of the surface layer-atmosphere interaction over land and water is available in Betts et al. (1996). Because of the nature of the hydrological cycle over

land, the precipitation (downdraft) efficiency needs to remain high (low) in order to attain a realistic hydrological budget over land.

For the experiments in this paper, therefore, the efficiency of convective downdraft is allowed to range from 0 to 1 over the ocean, as in nature (Fig. 1). This consideration also stems from the fact that weak vertical wind shear exists within the troposphere in the southern hemisphere where deep convection is favorably active, while shears increases northward where deep convection is inactive (Fig. 2). Over land, the upper limit of downdraft efficiency is limited to a prescribed value which depends upon model's horizontal resolution. For example, efficiency of the downdraft is less than 0.1 over land in a T40 grid resolution (about 300 km), and less than 0.2 at T62 (about 200 km). Another feature to be considered is the method of computing the vertical wind shears in (3). Tests are made where the top level of the vertical wind shear in (3) is changed from the maximum wind level below cloud top, to cloud top as originally constructed by Fritsch and Chappell (1980).

All the above considerations will be investigated, and experiments are summarized in Table 1. The control experiment (CNTL) employs the downdraft and evaporation efficiencies used in the operational convection scheme. Both downdraft and evaporation of precipitation are weakly parameterized. In particular, the impact of the evaporation efficiency (=0.07) on simulated precipitation is negligible. The DOWN experiment employs the relaxed downdraft over the ocean and suppressed over land, as proposed above. Note that the CNTL experiment and other experiments differ not only in the downdraft and evaporation efficiency but also in the determination of vertical wind shear within a cloud. The VTOP experiment, which employs the shear computation as in the operational scheme, is designed to clarify the sensitivity of precipitation forecasts to the method of computing the vertical wind shear. The LAND experiment employs the enhanced downdraft, not only over the ocean, but also over land, which in turn will highlights effects of the different surface-layer and atmosphere interactions. The EVAP experiment employs the enhanced evaporation efficiency of parameterized precipitation depending upon the vertical wind shear, as done in the DOWN experiment for downdraft efficiency. It is expected that the DOWN and EVAP experiments will simulate precipitation in a similar fashion, since the both downdraft and evaporation of precipitation reduce the convective precipitation by cooling and moistening the atmosphere.

The perpetual runs were initialized at 0000 UTC 15 January 1989 and integrated for 30 months with climatological SST data. The simulated climatology is determined by the lower boundary condition (SST), and the model physics and dynamics. The first six months are skipped to avoid uncertainties during the 'spinup' period, so the results shown in the following section will be an average of the final 24-months. To avoid unrealistic climate drift arising from the accumulation of snowfall during the integration period, the snowfall amount is reset to the January climatology on the first day of each month. A January SST climatology used in the model integration, together with the observed January precipitation climatology, are shown in Fig. 3. The SST is constructed from the monthly mean blended analyses of Reynolds (1988) during the 1950-1995 period. Observed January precipitation climatology is the average for 1979-1995 (Xie and Arkin 1996). Warm SST's appear between the Equator and 15S with a maximum in the central and western Pacific ocean, which is consistent with the precipitation distribution.

To avoid uncertainties in the perpetual run framework, five-member ensemble simulations were made for July 1996 and 1997, and January 1997 and 1998, with an approximate two-week

lead time. July and January ensembles started from 15, 16, 17, 18, and 19 June, and December, respectively. Initial data are taken from the NCEP/NCAR reanalysis (Kalnay et al. 1996). Observed SSTs are used to force lower boundary conditions. July 1996 and 1997 are regarded as Normal and El Nino summers in terms of SST anomalies over the central and eastern tropical Pacific, whereas January 1997 and 1998 are regarded as Normal and El Nino winters.

3. Results and discussion

a. Impact of modifications made to the downdrafts (CNTL versus DOWN)

Figure 4 compares the simulated precipitation climatology obtained from the CNTL and DOWN experiments. Overall, both experiments show precipitation climatology comparable to observed patterns, including two ITCZ's over the tropical ocean, precipitation associated with storm tracks over the midlatitude Pacific ocean and the western Atlantic ocean, and precipitation over the northwestern United States. Major differences are, however, found in the precipitation over the tropical oceans. It is apparent that the CNTL experiment has some discernible defects, including the excessive precipitation over the trade wind region north of the equator, weak precipitation activities over the southern Pacific warm pool region, and an isolated precipitation region over the western Indian ocean, all of which deviate significantly from climatology. Conversely, the results from the DOWN experiment clearly show considerable improvement. Spurious rainfall north of the equator is suppressed and the amount of rainfall in the Southern Hemisphere warm pool region is increased, leading to a better correlation with the SST distribution (Fig. 3a), particularly over the Pacific and Indian oceans. Over land, results are mixed. The increase of precipitation is apparent over Brazil and Australia in the DOWN experiment, which is partly due to the suppressed downdraft over land. On the other hand, the DOWN experiment still suffers from some undesirable features. A major deficiency is the underestimation of the precipitation amount over Indonesia, which seems related to the downstream impact of excessive precipitation appearing over the southern Indian ocean.

The modeled surface wind stress vectors are compared and verified against the observation in Figs. 5 and 6. Shaded areas designate a magnitude greater than 0.6 dyne/cm^2. Observed climatology (Fig. 5) is the average from 1966 to 1985 (Goldenberg and O'Brien 1981), which is available only over the Pacific ocean between 30S and 30N. Both experiments show general agreement with observations in terms of wind vector patterns, but appear to overestimate their magnitudes in strong wind regions. The DOWN experiment generally shows a better agreement with the observation, particularly in the Southern Hemisphere. A much closer agreement of the DOWN experiment to climatology is seen along the equator in the central Pacific. Additionally, the increase of easterlies east of Australia in the DOWN experiment is an improvement. In the two experiments and observations, southeasterlies from the southeastern Pacific merge with the northeasterly trade winds along the equator from 130 W-160 W. The strength of the easterlies in the DOWN experiment is much better than the weak easterlies in the CNTL experiment.

The 200-hPa zonal wind climatology from the two experiments are compared and verified with the observed (not shown). Overall, both experiments show quite good agreement with the observed climatology, including the midlatitude westerly jet stream in the Northern Hemisphere, the easterly wind over heavy precipitation regions in the Tropics, and strong westerly winds

associated with the Southern Hemisphere storm tracks. Differences between the two experiments appear in the Southern Hemisphere, where the precipitation difference is prominent. The overall similarities between the experiments suggest that the simulated large-scale climatology is weakly coupled to tropical convection. Such a weak coupling between the model dynamics and the equatorial convection has also been pointed out by Stephenson et al. (1998).

b. Further diagnoses of the impact of modified downdrafts

Since physical processes in the model are intimately related to each other, an explanation for the positive impact of the modifications made to the parameterized convection with DOWN experiment on the simulated climatology is not straightforward. Rather than describing the cause and effect for the differences, we begin by illustrating the direct impact of different precipitation mechanisms on model physics and then attempt to explain reason for the differences in resulting climatology. We focus on the diagnosis over the tropical Pacific ocean where the impact of enhanced downdraft is significant.

To illustrate the reasons why the DOWN experiment effectively reduces the precipitation north of the equator, the averaged vertical wind shear of horizontal wind is shown in Fig. 7. The convective portions of precipitation in the CNTL, DOWN and VTOP experiments are displayed in Fig. 8. The magnitude of the vertical wind shears is proportional to the downdraft efficiency (see section 2), so that strong wind shears will increase the downdraft intensity in the convective parameterization scheme (thus reducing precipitation). Note that the vertical wind shears shown in Fig. 7, are averages between 850 and 250 hPa. During a model integration, the values are averaged at sigma surfaces between the cloud base and cloud top, so that the distribution of wind shears in Fig. 7 is meaningful, but the magnitudes are less meaningful.

Despite these uncertainties, wind shears derived from the CNTL and DOWN experiments and observed data show similar characteristics, but wind shears from the DOWN experiment show a better agreement with the observations than these from the CNTL experiment (consistent with the improvement of precipitation climatology). However, to the north of the equator, where the CNTL experiment produces the erroneously excessive precipitation (Fig. 4a), relatively high wind shears appear in the both experiments and the observed data (Fig. 7). In particular, between 130W and 160W high wind shears are commonly diagnosed, which results in a reduction of convective rain in the DOWN experiment. From these comparisons, we can say that wind structures in that region are largely maintained by large scale circulations. Thus, the DOWN experiment efficiently reduces convective precipitation in that region even in the presence of the onset conditions to initiate deep convection.

In the Southern Hemisphere, all the experiments show relatively weak wind shears in the warm pool region, indicating that the direct impact of the modifications made in this study does not cause the increase of precipitation in that region (cf. Figs. 7b,c, and Figs. 8a,b). Rather, overall increase of precipitation amounts in the Southern Hemisphere from the DOWN experiment seems mostly due to the enhanced moisture fluxes into the region (cf. Fig. 6c). The increase of moisture flux over the warm pool region is apparently caused by a combination of reduced moisture loss to the surface and a change in the large-scale flow, both due to a reduction in deep convection in the northeast trade wind zone and along the ITCZ. In the CNTL experiment, deep convection is pronounced over the trade wind region, whereas in the DOWN experiment this convective activity is significantly suppressed by enhanced downdrafts in regions

of high wind shears. As pointed out by Ridout and Reynolds (1998), one possible mechanism creating the unrealistically low amount of warm pool precipitation in the CNTL experiment is dynamical suppression of low-level convergence over the region due to the occurrence of an excessive amount of deep convection north of equator.

To further investigate the impact of enhanced downdrafts, heating profiles of convective and large-scale precipitation for the CNTL and DOWN experiments are compared in Fig. 9. Shown in the figure are the sigma - longitude crosssections averaged over 0-15N. The convective parameterization scheme shows a maximum heating in the upper troposphere, while large-scale precipitation processes produce a maximum heating in the lower troposphere. Cooling in a below-cloud layer due to the downdrafts and evaporation of falling precipitates is evident. Allowing that the vertical extent of the heating distribution to represent cloud depth, one sees that parameterized convection (large-scale precipitation) process produces deep (shallow) clouds. The net heating distribution shows that the DOWN experiment destabilizes the bulk of the atmosphere more than the CNTL experiment, which is due to more larges-cale rain. The argument for precipitation efficiency in that region is in line with a recent observational study of Rauber et al. (1996). They showed that trade wind clouds are no more than 20-30 % efficient at returning evaporated water vapor to the ocean through precipitation processes.

Figure 10 shows the difference of sea level pressure between the two experiments (DOWN-CNTL). Again, a direct explanation to account for the large scale structure in relation to heating rates is not possible since the resulting climatology is a balanced system in which all physics interact with each other. It is seen that the DOWN experiment produces lower sea level pressure in the high SST region over the central and western Pacific and higher pressure in the eastern Pacific region than those from the CNTL experiment. This indicates an increase of the pressure gradient force northwestward from the southeastern Pacific. As a result, large scale circulation due to the differential heating feedback maintains a stronger Walker circulation in the DOWN experiment.

c. Impact of the method for calculation of vertical wind shear

It is evident that the simulated precipitation is quite sensitive to the method of computing the vertical wind shear within a cloud (Fig. 11). The VTOP experiment with the averaged shear between the cloud bottom and the maximum wind level below the cloud top shows a significant reduction of convective rainfall over the tropical ocean between 10S and 10N. This reduction of convection in the VTOP experiment is related to the location of maximum wind levels. As shown in Fig. 2, maximum wind levels can exist in the lower troposphere in the northeasterly trade wind regions, causing an increase of vertical wind shear over that region than in the DOWN experiment. However, this reduction of convective rain is partly offset by the significant amount of large-scale rain in the VTOP experiment (cf. Fig.8c). The ratio of convective rainfall to total precipitation over the tropical coean is about 80 % and 60 % for the DOWN and VTOP experiments, respectively. This large-scale rain in the VTOP experiment maybe due to undesirable feedback within below-cloud layers. Thus, when parameterized downdraft mass flux is strong, the downdraft can lift unstable air near the surface to PBL top, producing supersaturation (Hong and Pan 1998). Note that, though not shown, the amount of the precipitation anomaly is unrealistic in response to anomalous SST forcing when large-scale rain is pronounced.

d. Impacts of enhanced downdrafts over land

Figure 12 shows the precipitation difference between the DOWN and LAND experiments. It is noticeable that the enhanced downdraft over land weakens precipitation activities significantly, particularly in the Southern Hemisphere where most precipitation is due to parameterized convection. This is a demonstration of the different feedback of convection and surface hydrology over land and ocean. Over land, the convective activity depends upon the soil moisture which is related to the intensity of convection. Given the grid-scale forcing, the downdraft needs to be suppressed to provide a realistic feedback between the soil and atmosphere. This finding reinforces results from other studies (e.g., Spencer and Stensrud 1998) which showed the necessity of suppressing downdrafts to achieve realistic amounts of rainfall totals.

e. Downdraft versus re-evaporation of precipitation

In Fig. 13, we show the precipitation differences between the EVAP and CNTL experiments. It is evident that the enhanced evaporation of precipitation improves the simulated precipitation in a fashion similar to that of the enhanced downdraft (cf. Fig. 4c), which is not surprising given that the downdraft is an implicit representation for evaporation process in a convective cloud. Cooling and moistening rates due to evaporation are comparable to those from the DOWN experiment (not shown), but the magnitude for the EVAP experiment is smaller than in the DOWN experiment. Since parameterized downdrafts transport lower equivalent potential temperature air to lower levels, and since evaporative cooling alone would not change the equivalent potential temperature values, the potential stabilizing effect of the parameterized downdrafts is greater.

The above comparison implies that the improved oceanic precipitation climatology is primarily due to the use of the vertical wind shears within a cloud for controlling precipitation efficiency. Although modifications to either downdrafts or evaporation should be evaluated carefully, there are a few advantages to enhanced evaporation of falling precipitation in parameterized convection. For example, the enhanced evaporation process does not tend to produce undesirable feedback between the boundary layer and convection as in the case of strong downdrafts. When parameterized downdraft mass flux is strong, the downdraft can displace unstable air near the surface and lift it to its LCL and create this undesirable feedback. Indeed, excessive large-scale rain was simulated in a T62 resolution when convective downdrafts were maximized. Thus, enhanced evaporation has been used in the ensemble simulations shown in the following section.

f. Ensemble simulations

Figures 14 and 15 show observed and ensemble means of simulated precipitation for January 1997 and 1998, and July 1996 and 1997, respectively. Observed precipitation is from Xie and Arkin (1996). It can be seen that the model overestimates the precipitation amount. The observed global averages for the January 1997 and July 1996 are 2.86 mmd^{-1} and 3.01 mmd^{-1}, whereas the corresponding values are 3.56 mmd^{-1} and 3.66 mmd^{-1} for the CNTL, and 3.48 mmd^{-1} and 3.60 mmd^{-1} for the EVAP experiments. The reduction of the precipitation in the EVAP is due to suppressed convective activities over the oceans.

To assess the reliability of simulations, we performed a statistical t-test on each grid. Each member of the ensemble is considered as one degree of greedom. The procedure can be found in Masutani and Leetmaa (1999). Areas where values are statistically significant at the 95 % level are shaded in the simulated precipitation. In the winter experiments (Fig. 14), it can be seen that the EVAP experiment improves precipitation over the tropical oceans. The improvement for the normal winter case (January 1997) is comparable to what was seen in the perpetual run (Fig. 4). Excessive rainfall north of the equatorial Pacific is significantly reduced and precipitation over the western Pacific warm pool region is also improved. For the El Nino winter case (January 1998), the both CNTL and DOWN experiments show a general agreement with the observed, but the simulated precipitation from the DOWN experiment is statistically more significant than in the CNTL.

Although our motivation of this study is to improve the deficiencies of tropical precipitation during the northern Hemispheric winter, the improvement is striking for the summers (Fig. 15). A serious rainfall deficit over the western pacific warm pool region for both summers is significantly improved when enhanced evaporation is introduced. For a normal summer (July 1996), the precipitation amount over the western Pacific warm pool region is increased in the EVAP experiment. Although the EVAP experiment underestimates precipitation amount in Indonesia, the distribution of precipitation and its statistical significance are much better than those from the CNTL experiment.

Precipitation anomalies between the two years are significantly improved in the EVAP experiment, for both winters and summers (Fig. 16). In the CNTL, the winter precipitation anomalies over the Pacific reveal too strong meridional gradient, with positive anomaly displaced eastward. The EVAP experiment improves this deficiency. The overall improvement is prominent over the Indian ocean. However, the anomalies over the Indonesian region are still weak. As shown in mean climatology for summers (Fig. 15), improvement of anomalies is pronounced for summer cases. A strong El Nino signal in 1997 summer with positive anomalies in central and eastern Pacific are better simulated when enhanced evaporation is introduced.

4. Concluding remarks

It has been illustrated that simulated climatology is quite sensitive to the intensity of downdraft efficiency and its specifications in parameterized convection, as found by previous studies in mesoscale modeling area. Although the success of simulated climatology with enhanced downdraft and evaporation over the oceans is clear, it is important to realize the uncertainties in the inverse relationship between vertical wind shear and downdraft mass flux. While there is some correlation between wind shear and precipitation efficiency (and then some correlation between precipitation efficiency and downdraft mass flux), there is little evidence for a specific quantitative relationship (Knupp and Cotton 1985). Despite these uncertainties our results give some important implications on the representation of parameterized convection. First, coupling cloud properties to dynamic quantities, such as the vertical wind shears, can improve simulated climatology. A notable approach in this study is to relax downdraft or evaporation efficiency up to

the theoretical limits, 100 %, over the oceans. This is contradictory to the arguments in previous studies (e.g., Spencer and Stensrud 1998) who minimized the efficiencies to improve quantitative precipitation forecasts. This implies that an insight into different surface layer-atmosphere interaction over water and land can help in parameterizing cloud properties. The proposed enhanced evaporation of precipitation became operational in NCEP's global model, in June 1998.

Acknowledgments. The author is grateful to Hua-Lu Pan, Arun Kumar for useful discussions. Thanks go to Ken Campana and Joe Gerrity for helpful editorial suggestions.

References

Arakawa, A. and W. H. Shubert, 1974: Interaction of a cumulus ensemble with the large-scale environment, Part I. *J. Atmos. Sci.*, 31, 674-704.

Baik, J.J., M. Takahashi, 1995: Sensitivity fo the GCM-simulated large-scale structures to two cumulus parameterizations. J. Meteor. Soc. Japan, 73, 975-991.

Betts, A. K., J.H. Ball, A.C.M. Beljaars, M.J. Miller, and P.A. Viterbo, 1996: The land surface-atmospheric interaction: A review based on observational and global modeling perspectives. *J. Geophys. Res.*, 101, 7209-7225.

Caplan, P., J. Derber, W. Gemmill, S.-Y. Hong, H.-L. Pan, and D. Parrish, 1997: Changes to the 1995 NCEP operational medium-range forecast model analysis-forecast system. *Wea. and Forecasting*, 12, 581-594.

Cheng, M.-D., and A. Arakawa, 1997: Inclusion of rainwater budget and convective downdrafts in the Arakawa-Schubert cumulus parameterization. J. Atmos. Sci., 54, 1359-1378.

Frank, W. M., and C. Cohen, 1987: Simulation of tropical convective systems. Part I: A cumulus parameterization. J. Atmos. Sci., 44, 3787-3799.

Fritsch, J. M. and C.F. Chappell, 1980 : Numerical prediction of convectively driven mesoscale pressure systems. Part I: Convective parameterization. *J. Atmos. Sci.*, 37, 1722-1733.

Gates, W. L., 1992: AMIP: Atmospheric Model Intercomparison Project. *Bull. Amer. Meteor. Soc.*, 73, 1962-1970.

Giorgi, F., M. R. Marinucci, G.T. Bates, and G.D. Canio, 1993: Development of a second-generation regional climate model (RegCM2). Part II: Convective processes and assimilation of lateral boundary conditions. *Mon. Wea. Rev.*, 121, 2813-2832.

Goldenberg, S. D., and J.J. O'Brien, 1981 : Time and space variability of tropical Pacific wind stress. *Mon. Wea. Rev.*, 109, 1190-1207.

Grell, G. A., 1993 : Prognostic evaluation of assumptions used by cumulus parameterization. *Mon. Wea. Rev.*, 121, 764-787.

Hong S.-Y. and H.-L. Pan, 1996 : Nonlocal boundary layer vertical diffusion in a medium-range forecast model. *Mon. Wea. Rev.*, 124, 2322-2339.

_____, and _____, 1998 : Convective trigger function for a mass flux cumulus parameterization scheme. *Mon. Wea. Rev.*, 126, 2599-2620.

Johnson, R.H., 1976: The role of convective-scale precipitation downdrafts in cumulus and synoptic-scale interactions. *J. Atmos. Sci.*, 33, 1890-1910.

Kain, J.S, and J.M. Fritsch, 1990: A one-dimensional entraining/detraining plume model and its application in convective parameterization. J. Atmos. Sci., 47, 2784-2802.

Kalnay, E. and Coauthors, 1996 : The NCEP/NCAR 40-year reanalysis project. *Bull. Amer. Meteor. Soc.*, 77, 437-471.

Kanamitsu, M., 1989: Description of the NMC global data assimilation and forecast system. *Wea. and Forecasting*, 4, 335-342.

_____, and Coauthors, 1991: Recent changes implemented into the global forecast system at NMC. *Wea. and Forecasting*, 6, 425-435.

Kessler, E., 1969: *On the distribution and continuity of water substance in atmospheric circulations.* American Meteoro. Soc., Meteor. Monograph 10, No 32, 84 pp.

Knupp, K.R., and W. R. Cotton, 1985: Convective cloud downdraft structure: An interpretive survey. *Rev. Geophys.*, 23, 183-215.

Kumar, A., M. Hoerling, M. Ji, A. Leetmaa, and P. Sardeshmukh, 1996: Assessing a GCM's suitability for making seasonal predictions. *J. Climate*, 9, 115-129.

Lord, S. J. 1978: Development and observational verification of a cumulus cloud parameterization from the anvil clouds of deep tropical convection. Ph. D. Dissertation, University of California, Los Angeles, 359 pp. [Available from UCLA, Los Angeles, CA 90024].

Masutani, M. 1997 : Relation between SST and rainfall on the seasonal time scale. *Proceedings of the twenty-second annual climate diagnostics and prediction workshop.* E. O. Lawrence Berkeley National Laboratory of California, Berkeley, California, October 6-10. 65-68. [Available from Climate Prediction Center, NCEP, 5200 Auth Road, Camp Springs MD 20746]

_____, and A. Leetmaa 1999: Dynamical mechanisms of the 1995 California floods. J. Climate, in press.

Molinari, J., and T. Corsetti, 1985: Incorporation of cloud-scale and mesoscale downdrafts into cumulus parameterization: Results of one- and three-dimensional integrations. *Mon. Wea. Rev.*, 113, 485-501.

NMC Development Division, 1988: Documentation of the research version of the NMC Medium-Range Forecasting Model, 504 pp. [Available from NCEP/EMC, 5200 Auth Road, Camp Springs MD 20746]

Pan, H.-L., and L. Mahrt, 1987: Interaction between soil hydrology and boundary layer developments. *Boundary-Layer Meteor.*, 38, 185-202.

_____, and W.-S. Wu, 1995: Implementing a mass flux convective parameterization package for the NMC medium-range forecast model. NMC office note 409, 40 pp. [Available from NCEP/EMC, 5200 Auth Road, Camp Springs MD 20746]

Rauber, R. M., N. F. Laird, and H. T. Ochs III, 1996 : Precipitation efficiency of trade wind clouds over the north central tropical Pacific ocean. *J. Geophys. Res.*, 101, 26247-26253.

Reynolds, R. W., 1988 : A real-time global sea surface temperature analysis. *J. Climate,* 1, 75-86.

Ridout, J., and C. A. Reynolds, 1998 : Western pacific warm pool region sensitivity to convective triggering by boundary layer thermals in the NOGAPS atmospheric GCM. J. Climate, 11, 1553-1573.

Sela, J., 1980: Spectral modeling at the National Meteorological Center. *Mon. Wea. Rev.*, 108, 1279-1292.

Spencer, P.L., and D.J. Stensrud, 1998: Simulating flash flood events: Importance of the subgrid representations of convection. Mon. Wea. Rev., 126, 2884-2912.

Stephenson, D.B, F. Chauvin, J.-F. Royer, 1998: Simulation of the Asian summer monsoon and its dependence on model horizontal resolution. *J. Meteor. Soc. Japan*, 76, 237-265.

Wang, W. and N. Seaman, 1997 : A comparison study of convective parameterization schemes in a mesoscale model. *Mon. Wea. Rev.*, 125, 252-278.

Xie, P. and P. A. Arkin, 1996: Analyses of global monthly precipitation using gauge observations, satellite estimates, and numerical model predictions. *Climate*, 9, 840-858.

Xu, K.-M., and A. Arakawa, 1992: Semiprognostic tests of the Arakawa-Schubert cumulus parameterization using simulated data. *J. Atmos. Sci.,* 49, 2421-2436.

Zhang, D.-L., and M. Fritsch, 1986: Numerical simulation of the meso-β scale structure and evolution of 1977 Johnstown flood. Part I: Model description and verification. *J. Atmos. Sci.*, 43, 1913-1943.

_____, and K. Gao, 1989 : Numerical simulation of an intense squall line during 10-11 June 1985 PRE-STORM. Part II: Rear inflow, surface pressure perturbations and stratiform precipitation. *Mon. Wea. Rev.*, 117, 2067-2094.

Zhang, G. J., 1995: The sensitivity of surface energy balance to convective parameterization in a general circulation model. *J. Atmos. Sci.*, 52, 1370-1382.

Zipser, E.J., 1977 : Mesoscale and convective-scale downdrafts as distinct components of squall-line structure. Mon. Wea. Rev., 105, 1568-1589.

Table 1. Summary of experimental designs

Experiment	Code	β	α	Top level of the vertical wind shear
Perpetual runs	CNTL	0 to 0.3 over ocean and land	0.07 over ocean and land	Maximum wind level within the cloud
	DOWN	0 to 1.0 over ocean , 0 to 0.1 over land	0.07 over ocean and land	Cloud top
	VTOP	0 to 1.0 over ocean , 0 to 0.1 over land	0.07 over ocean and land	Maximum wind level within the cloud
	LAND	0 to 1.0 over ocean and land	0.07 over ocean and land	Cloud top
	EVAP	0 over ocean and land	0 to 1.0 over ocean, 0 over land	Cloud top
Ensemble runs	CNTL	0 to 0.3 over ocean and land	0.07 over ocean and land	Maximum wind level within the cloud
	EVAP	0 over ocean and land	0 to 1.0 over ocean, 0 over land	Cloud top

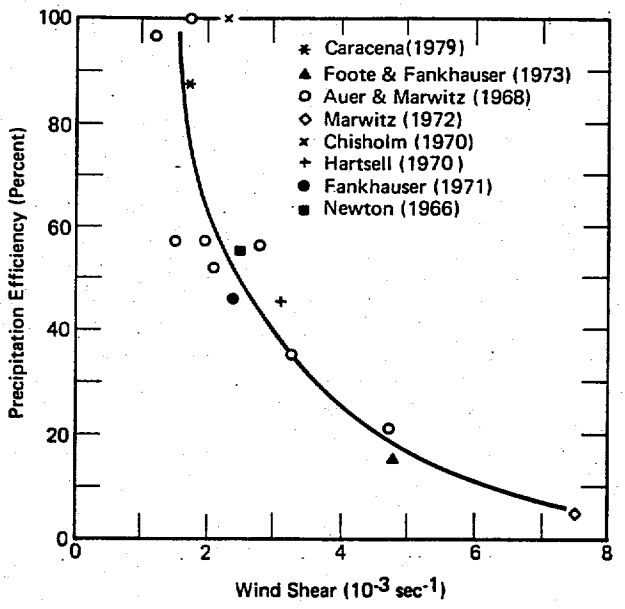

Fig. 1. Precipitation efficiency (ratio of rainout to water vapor inflow) as a function of vertical shear of the horizontal wind in the layer from cloud base to cloud top [from Fritch and Chappell(1980)].

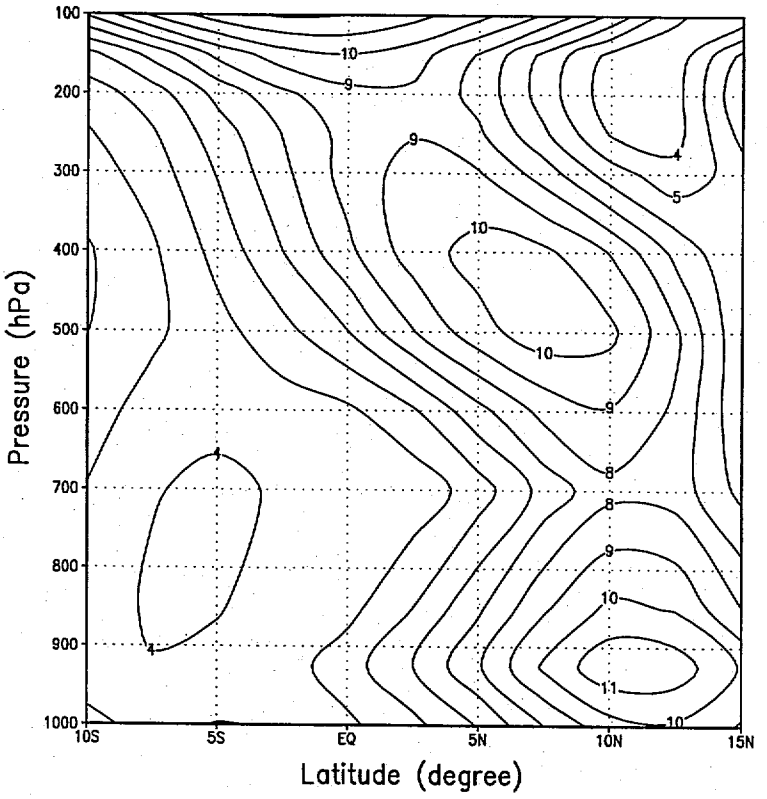

Fig. 2. Pressure-latitude crosssection of the January wind speed climatology (ms^{-1}) along 170 E, averaged from1979 and 1996.

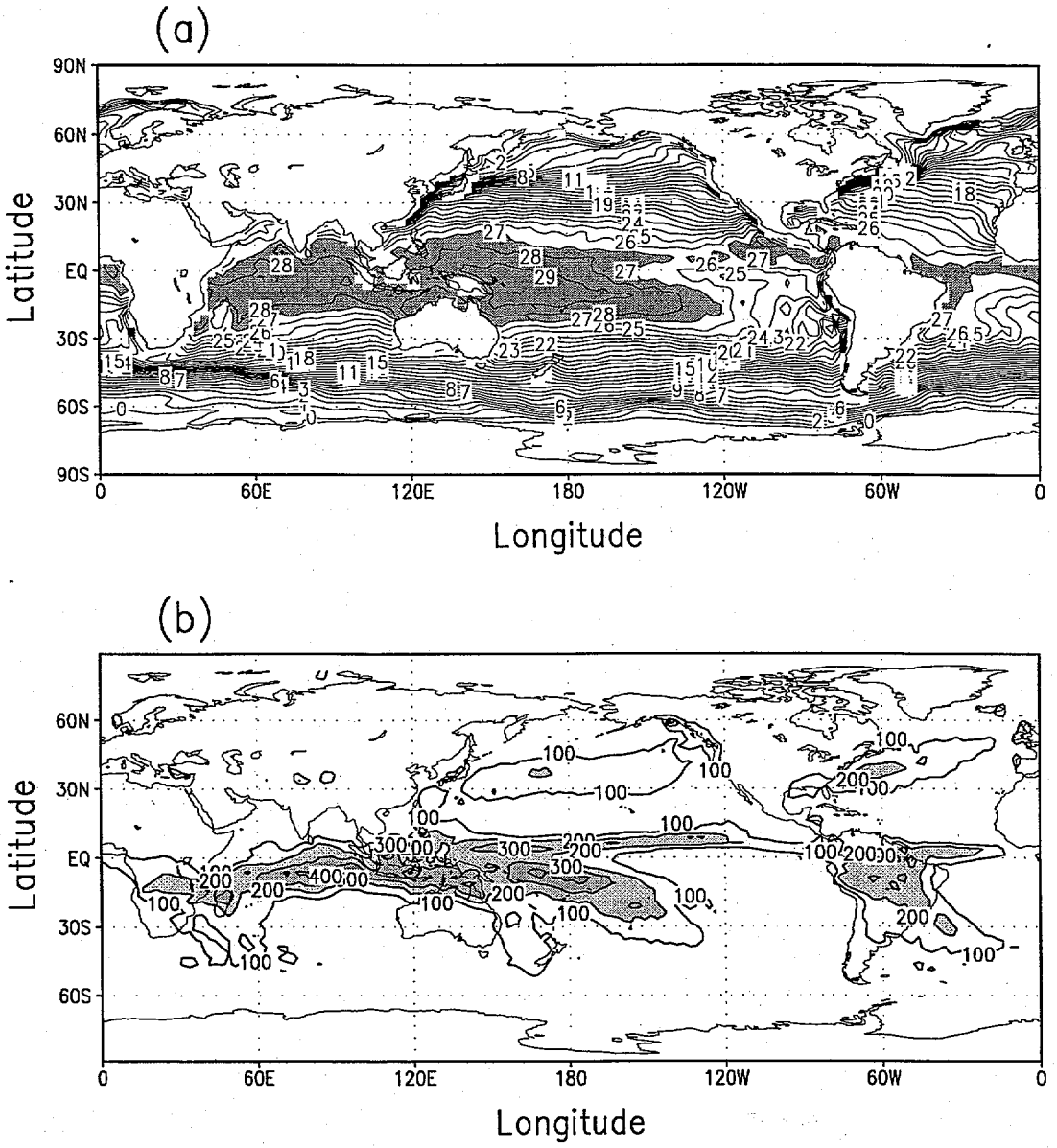

Fig. 3. (a) Sea surface temperature (C) and (b) precipitation (mm) climatology for January.

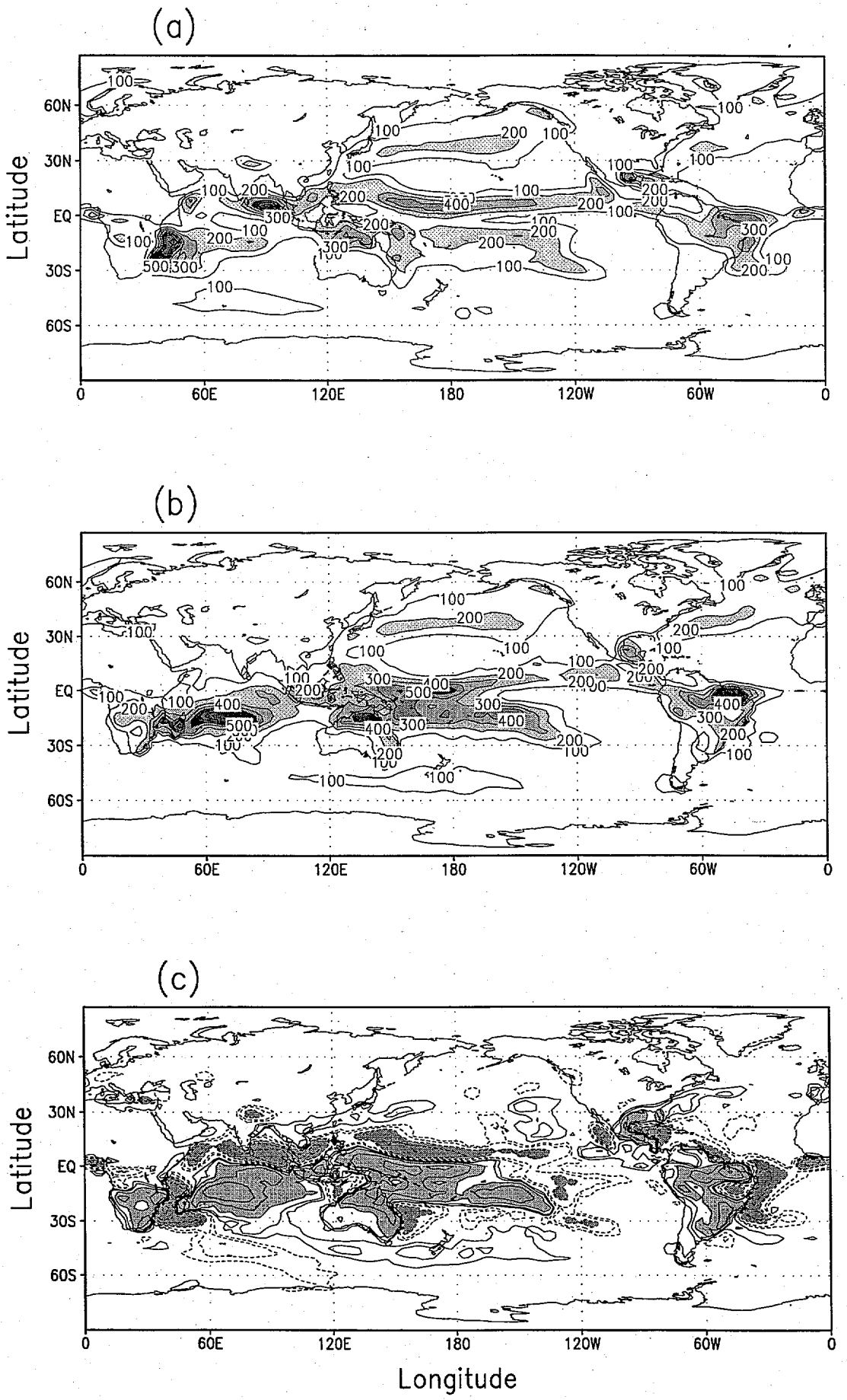

Fig. 4. Simulated precipitation from the (a) CNTL and (b) DOWN experiments, and the difference (DOWN-CNTL). Contour in (c) are± 20, ± 40, ± 80, ± 160, ± 320. Shaded in (c) are the absolute values over 80 mm.

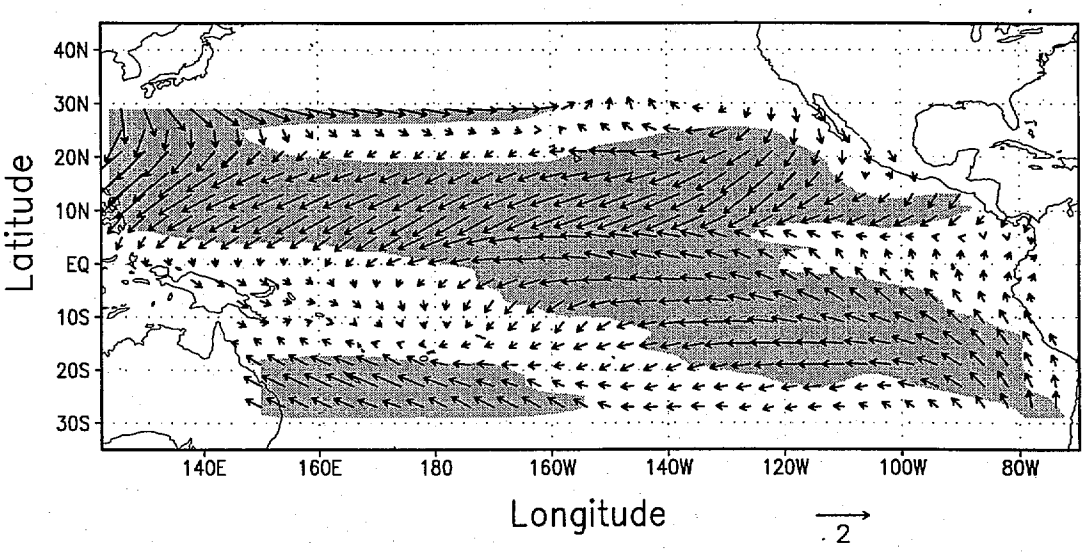

Fig. 5. Observed surface stress vectors (dynecm^{-2}). Wind vectors are plotted every two grid points. Size of vector is represented in the arrow at the right bottom of figure. Shaded areas designate the magnitude greater than 0.6 dynecm^{-2}.

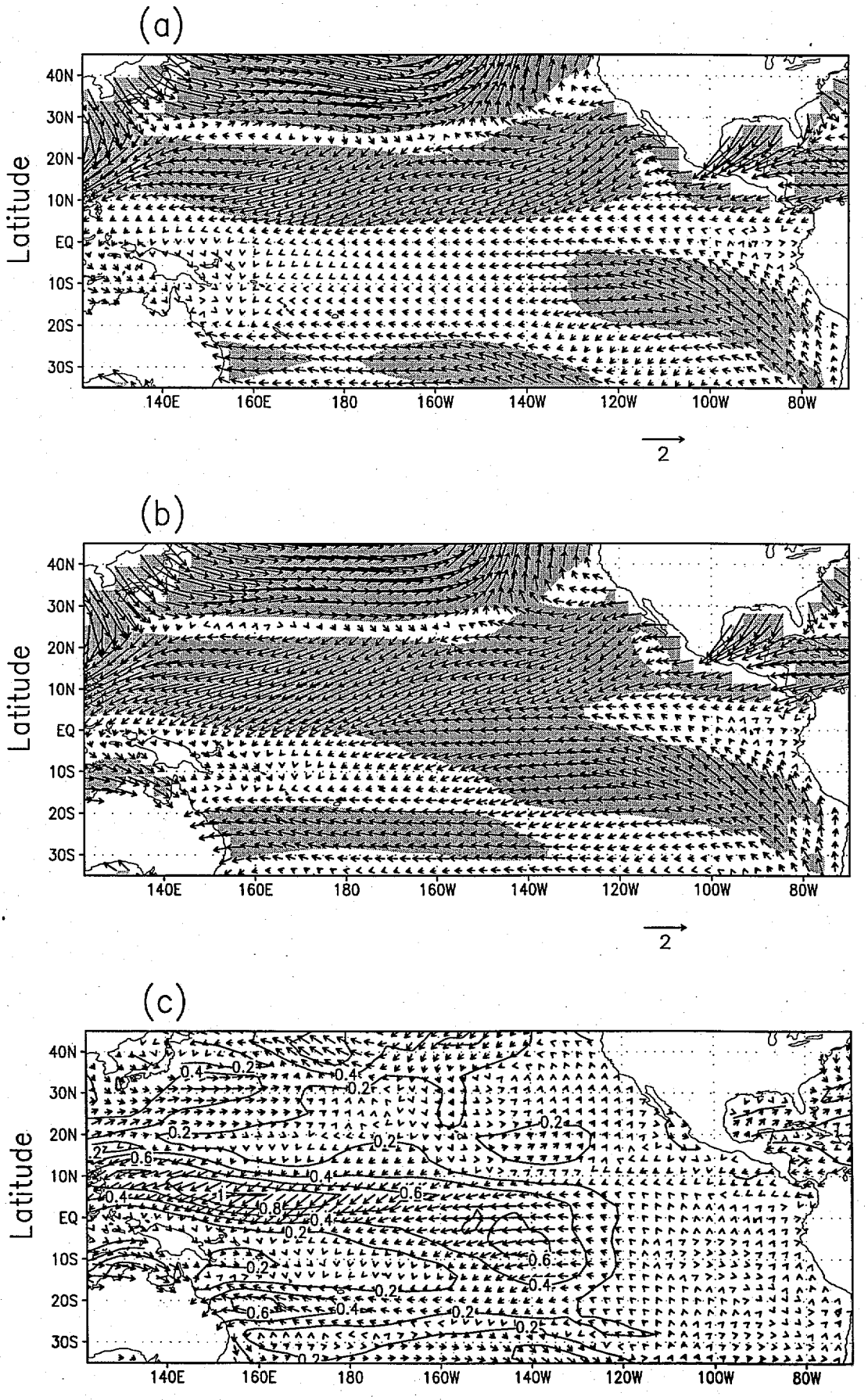

Fig. 6. As in Fig. 5 but for the simulations from the (a) CNTL, (b) DOWN experiments, and (c) the difference (DOWN-CNTL).

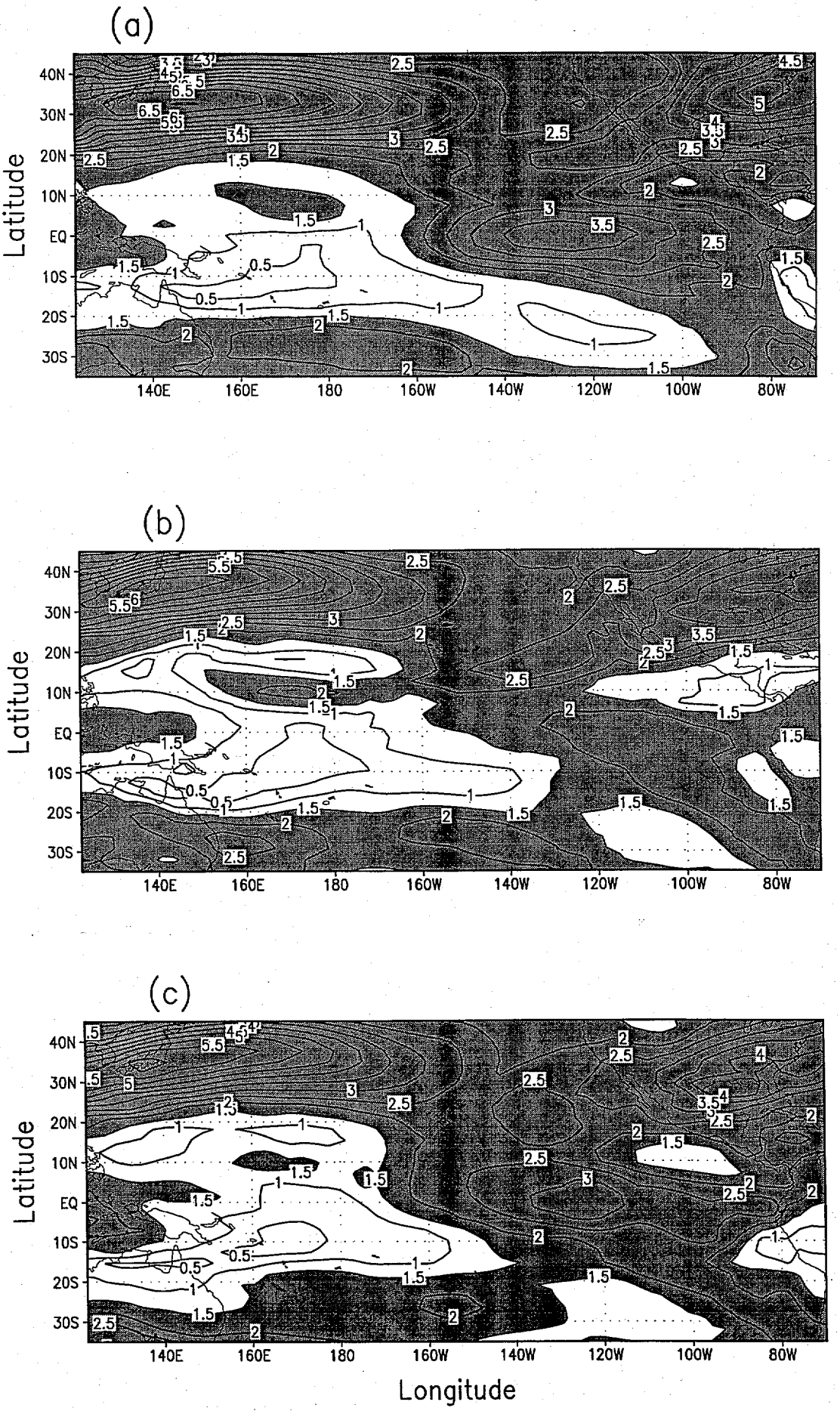

Fig. 7 (a) Observed vertical wind shears of the horizontal wind, and the corresponding model simulations from the (b) CNTL and (c) DOWN experiments. Shaded areas designate their magnitude greater than 1.5 s^{-1}.

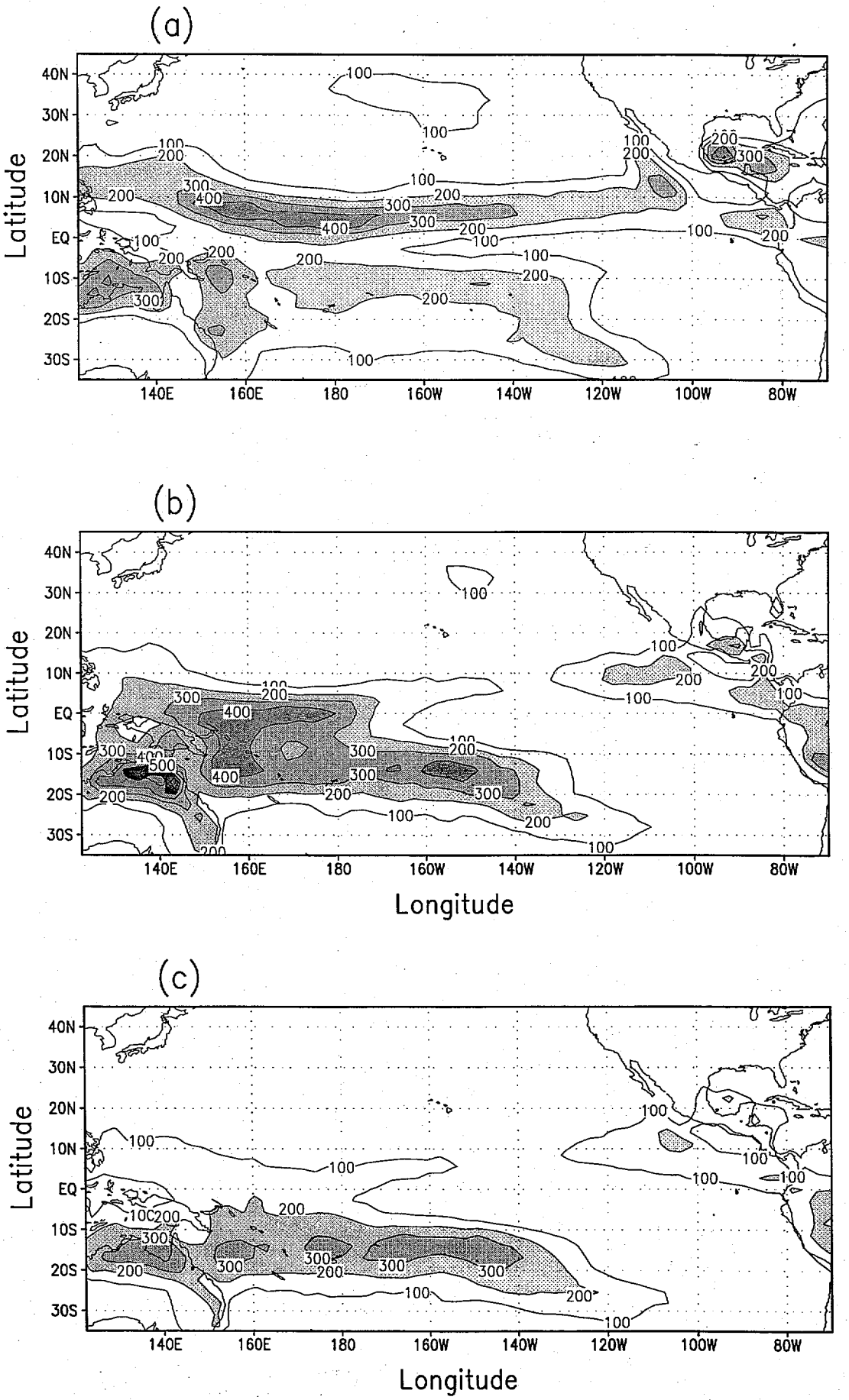

Fig. 8. Comparison of convective precipitation resulted from the (a) CNTL, (b) DOWN, and (c) VTOP experiments.

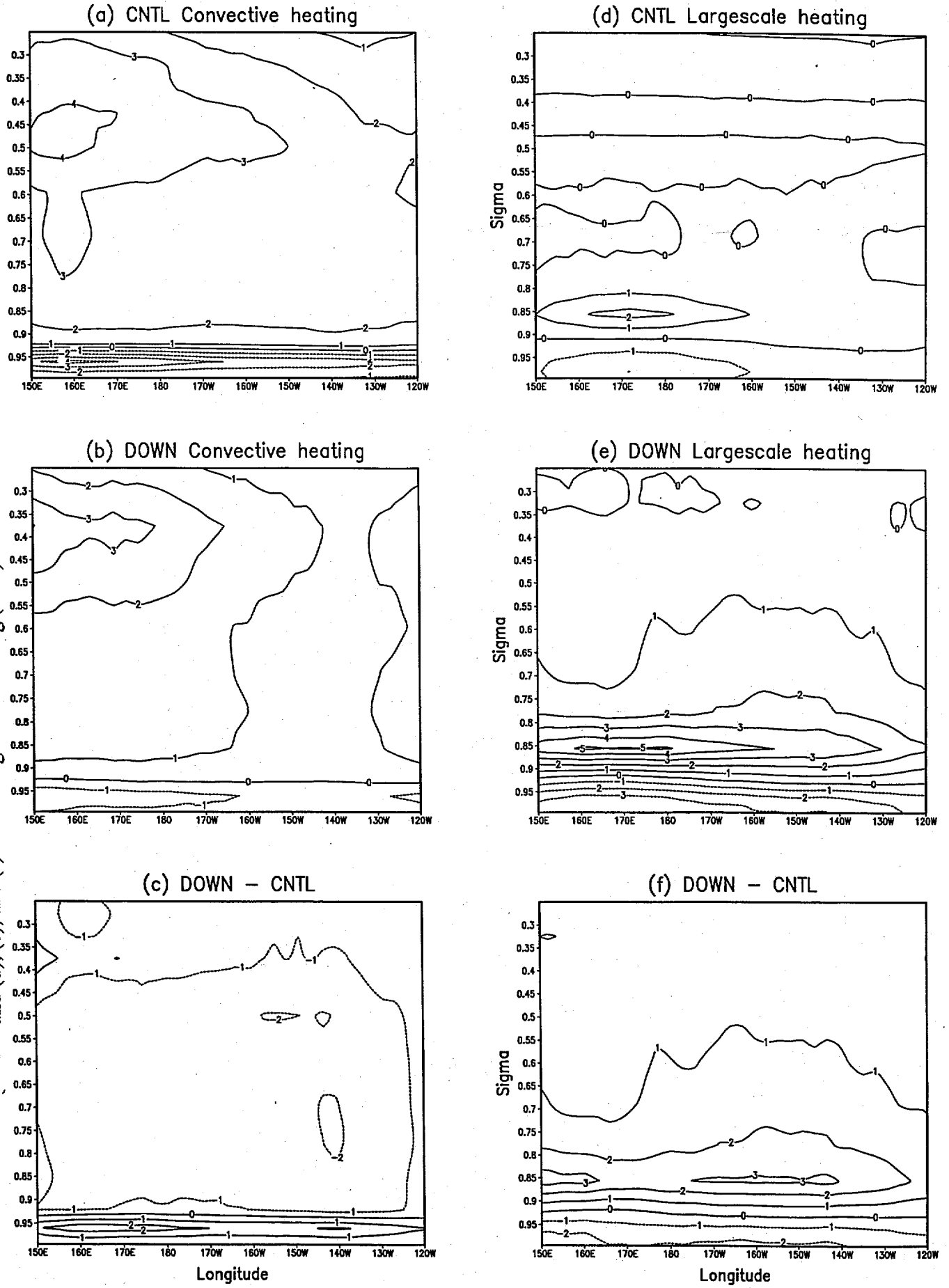

Fig. 9. Comparison of sigma-longitude cross-sections, averaged between equator and 15 N, of convective heating from the (a) CNTL, (b) DOWN, and (c) the difference (DOWN-CNTL), and (d), (e), and (f) for the large-scale heating (Kd^{-1}).

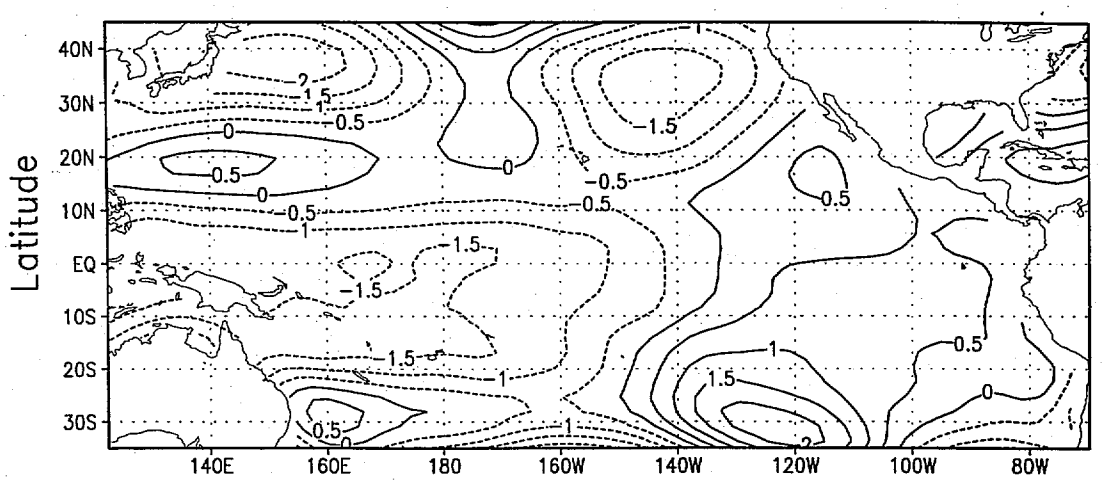

Fig. 10. Difference of simulated sea level pressure climatologies (hPa) (DOWN-CNTL).

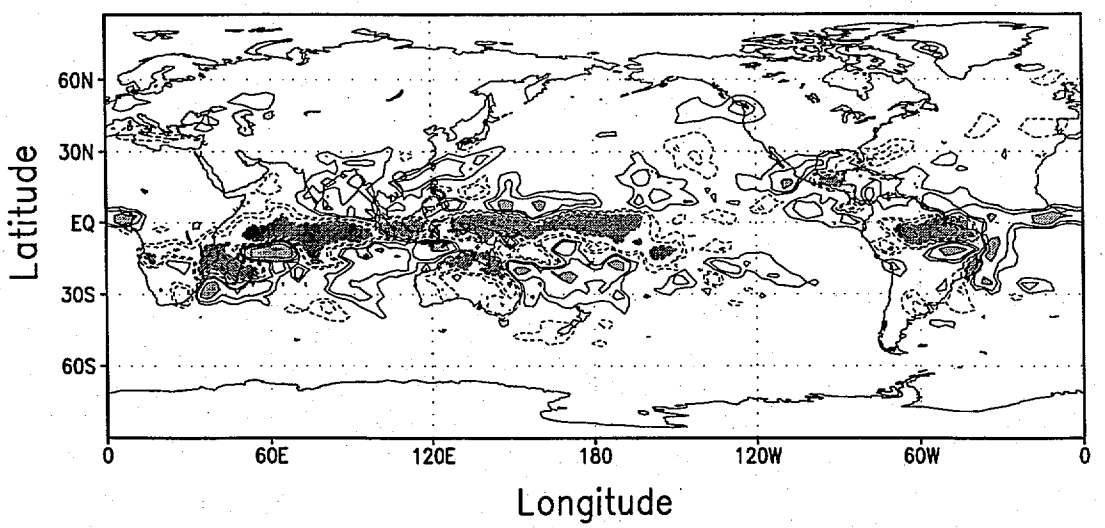

Fig. 11. Same as in Fig. 4c, but for the difference (VTOP-DOWN).

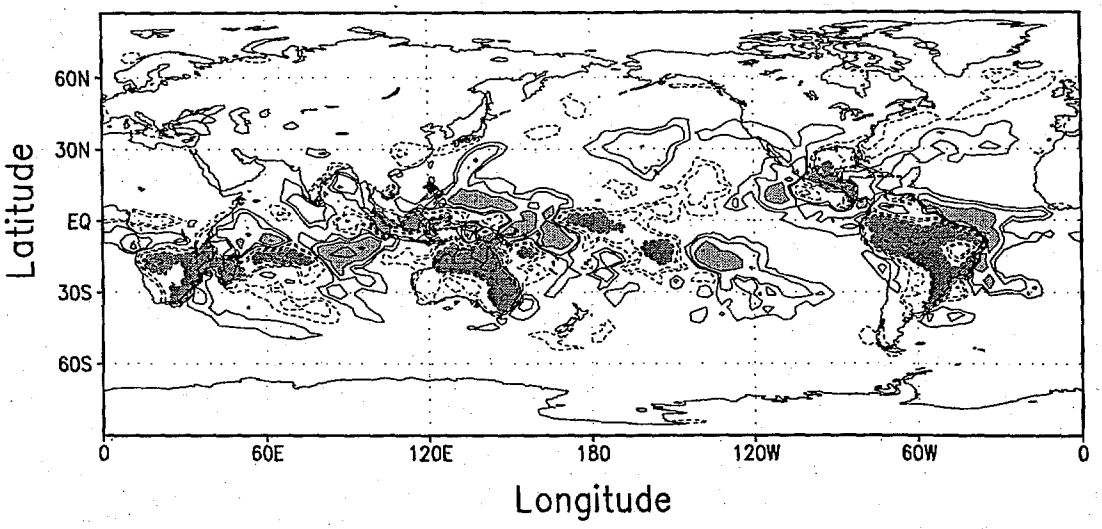

Fig. 12. Same as in Fig. 4c, but for the difference (LAND-DOWN).

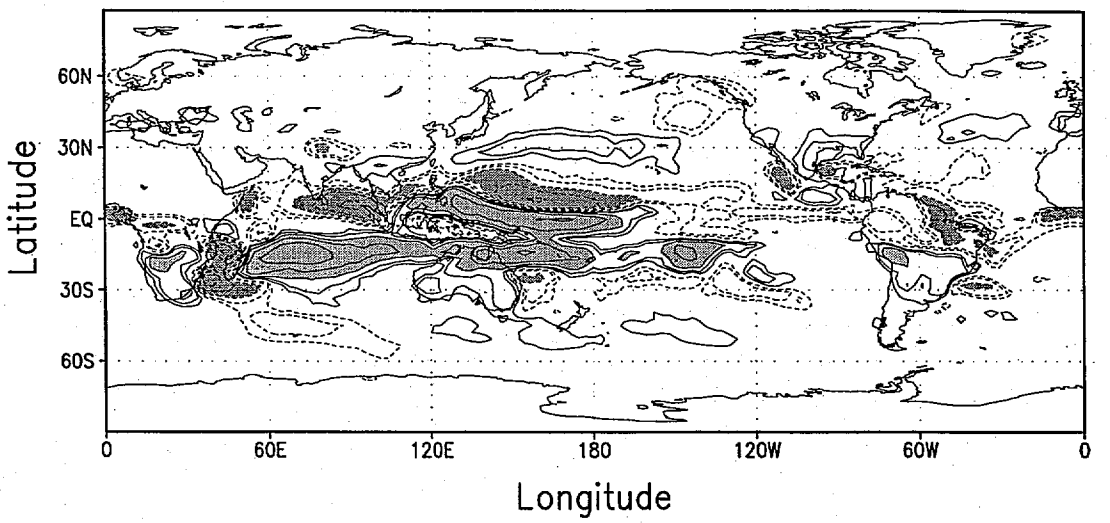

Fig. 13. As in Fig. 4c, but for the difference (EVAP-CNTL).

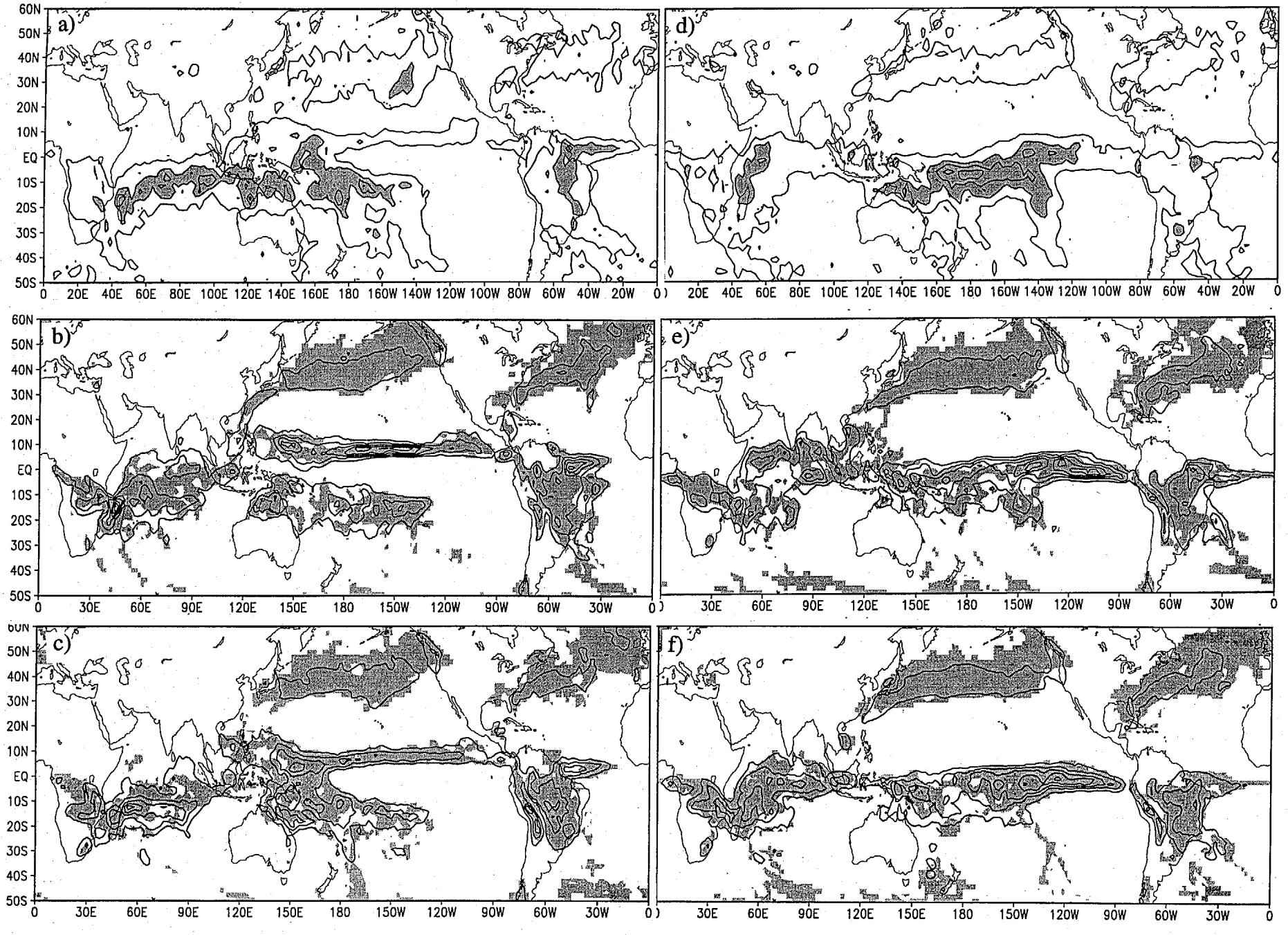

Fig. 14. Comparison of observed (upper) and simulated precipitation from the CNTL (middle), and EVAP (bottom) experiments, for January 1997 (a,b,c) and 1998 (d,e,f). Contour intervals are 200 mm starting from 100 mm. Shaded in observed precipitation, (a) and (d), designate the precipitation amount greater than 200 mm. Areas where values are statistically significant at the 95 % level are shaded, for the simulated results, (b), (c), (e), and (f).

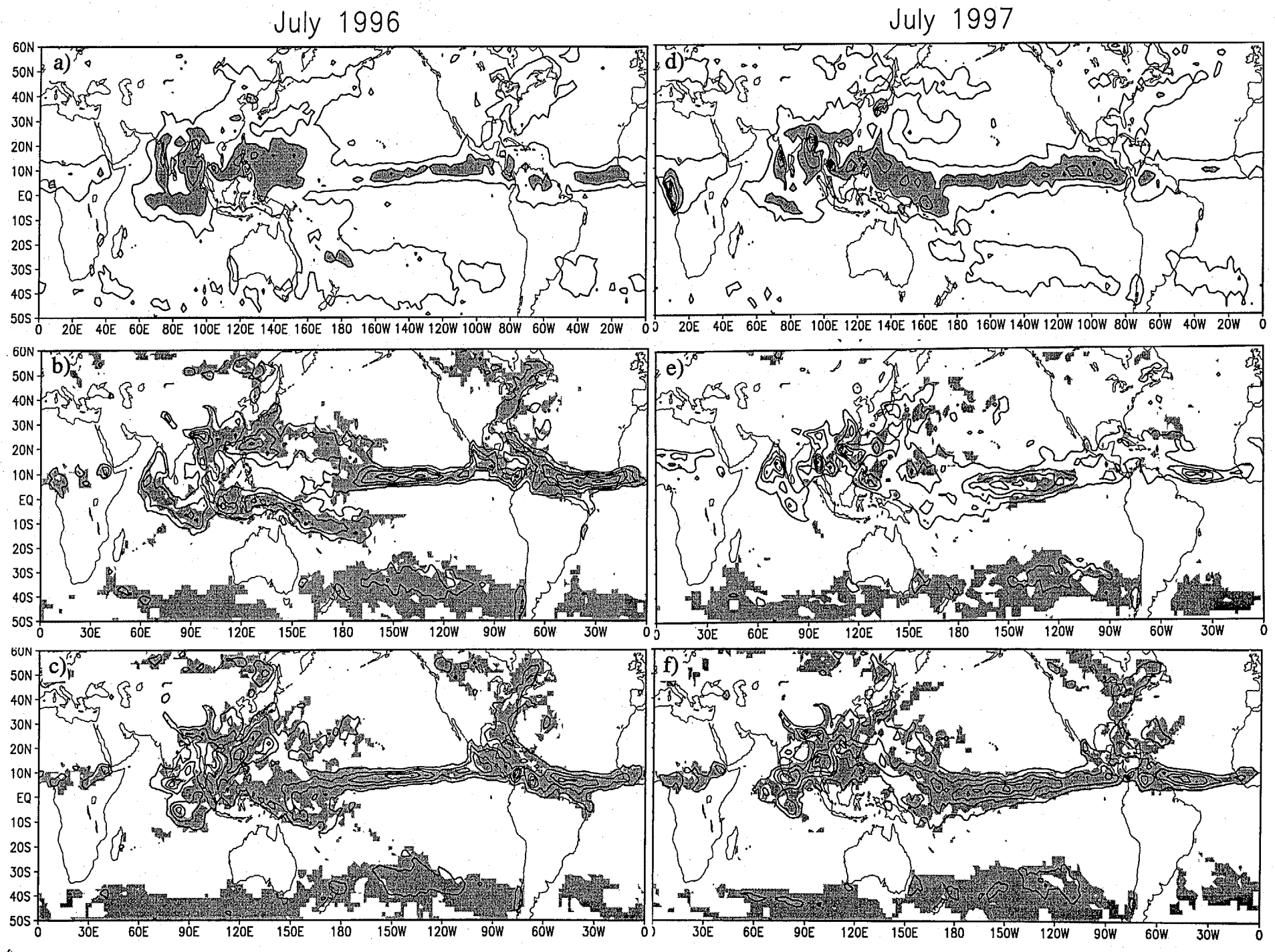

Fig. 15. As in Fig. 14, but for the summer cases, July of 1996 (a,b,c) and 1997 (d,e,f).

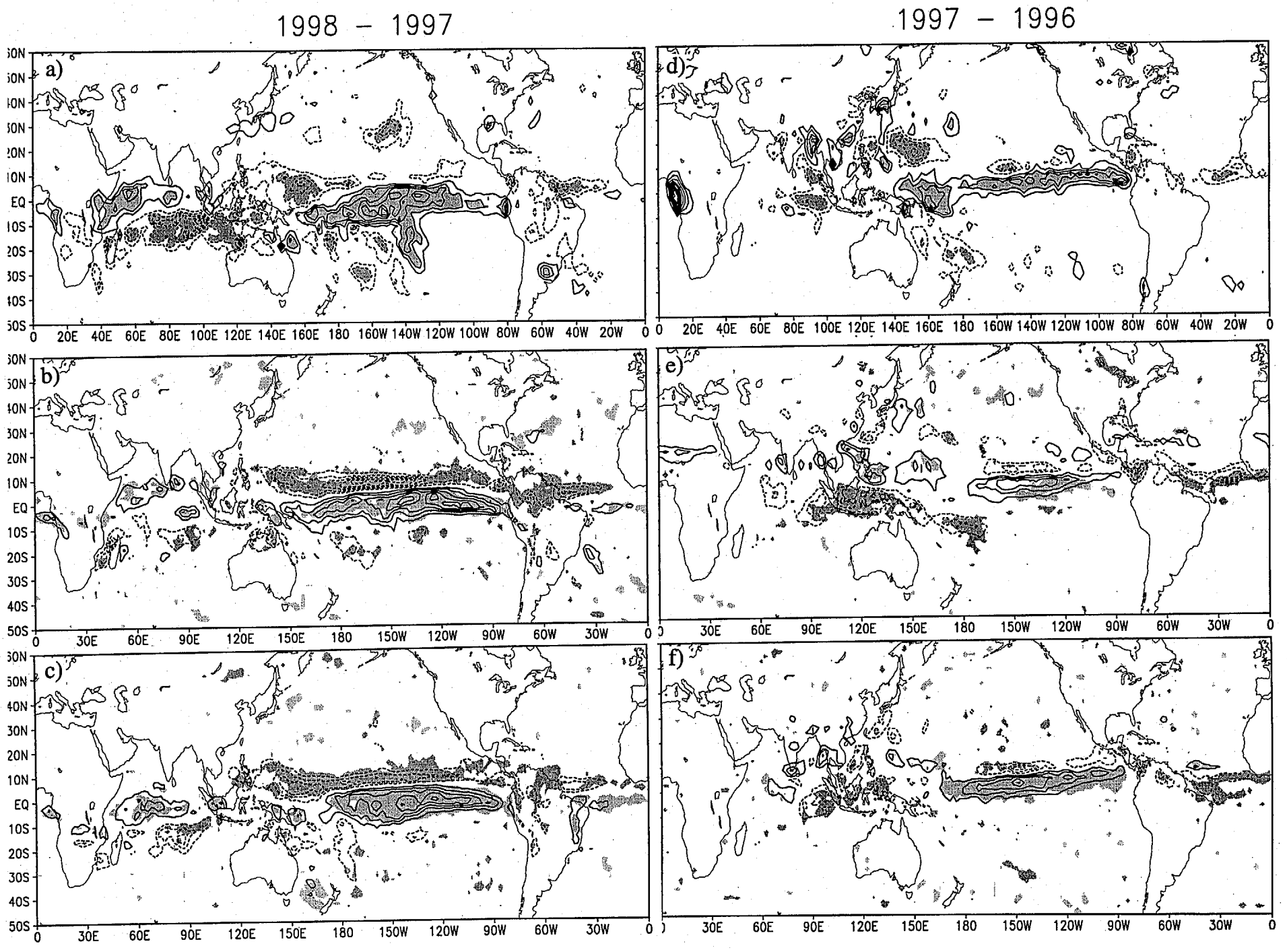

Fig. 16. As in Fig. 14, but for the anomalies, for January (1998-1997) (a,b,c), and July (1997-1996) (d,e,f).